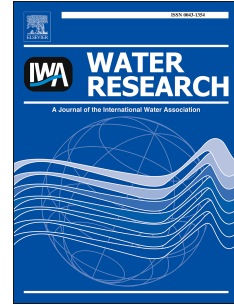


# Accepted Manuscript

High-solids anaerobic digestion model for homogenized reactors

Vicente Pastor-Poquet, Stefano Papirio, Jean-Philippe Steyer, Eric Trably, Renaud Escudié, Giovanni Esposito



PII: S0043-1354(18)30460-3

DOI: [10.1016/j.watres.2018.06.016](https://doi.org/10.1016/j.watres.2018.06.016)

Reference: WR 13843

To appear in: *Water Research*

Received Date: 19 March 2018

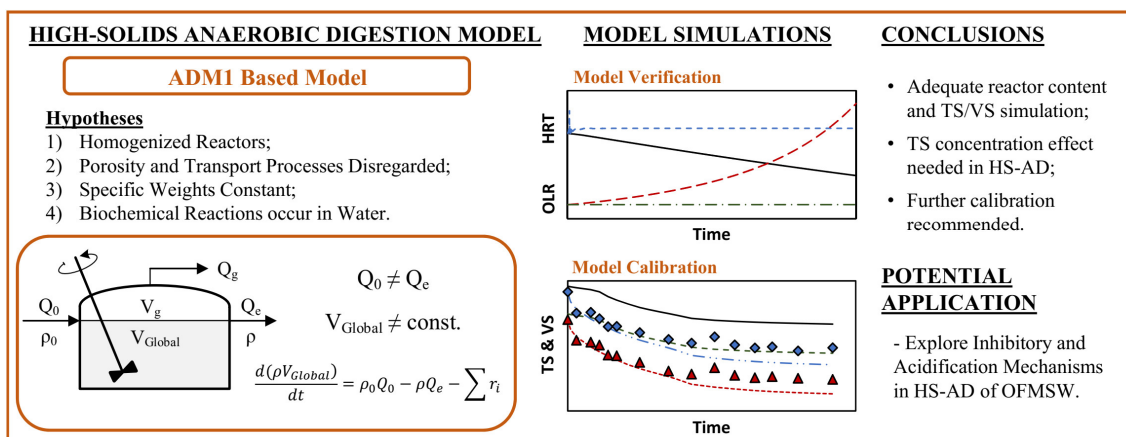
Revised Date: 22 May 2018

Accepted Date: 7 June 2018

Please cite this article as: Pastor-Poquet, V., Papirio, S., Steyer, J.-P., Trably, E., Escudié, R., Esposito, G., High-solids anaerobic digestion model for homogenized reactors, *Water Research* (2018), doi: 10.1016/j.watres.2018.06.016.

This is a PDF file of an unedited manuscript that has been accepted for publication. As a service to our customers we are providing this early version of the manuscript. The manuscript will undergo copyediting, typesetting, and review of the resulting proof before it is published in its final form. Please note that during the production process errors may be discovered which could affect the content, and all legal disclaimers that apply to the journal pertain.

## Graphical Abstract



1 **High-Solids Anaerobic Digestion Model for Homogenized Reactors**

2

3 Vicente Pastor-Poquet <sup>a,b,\*</sup>, Stefano Papirio <sup>c</sup>, Jean-Philippe Steyer <sup>b</sup>, Eric Trably <sup>b</sup>,

4 Renaud Escudié <sup>b</sup>, and Giovanni Esposito <sup>a</sup>

5

6 <sup>a</sup> Department of Civil and Mechanical Engineering, University of Cassino and Southern

7 Lazio, via Di Biasio 43, 03043 Cassino (FR), Italy

8 \*Corresponding author. E-mail: [vicente.pastor.poquet@gmail.com](mailto:vicente.pastor.poquet@gmail.com)

9 <sup>b</sup> LBE, Univ Montpellier, INRA, 102 avenue des Etangs, 11100, Narbonne, France

10 <sup>c</sup> Department of Civil, Architectural and Environmental Engineering, University of

11 Napoli Federico II, via Claudio 21, 80125 Napoli, Italy

12

**13 ABSTRACT**

14 During high-solids anaerobic digestion (HS-AD) of the organic fraction of municipal  
15 solid waste (OFMSW), an important total solid (TS) removal occurs, leading to the  
16 modification of the reactor content mass/volume, in contrast to ‘wet’ anaerobic  
17 digestion (AD). Therefore, HS-AD mathematical simulations need to be approached  
18 differently than ‘wet’ AD simulations. This study aimed to develop a modelling tool  
19 based on the anaerobic digestion model 1 (ADM1) capable of simulating the TS and the  
20 reactor mass/volume dynamics in the HS-AD of OFMSW. Four hypotheses were used,  
21 including the effects of apparent concentrations at high TS. The model simulated  
22 adequately HS-AD of OFMSW in batch and continuous mode, particularly the  
23 evolution of TS, reactor mass, ammonia and volatile fatty acids. By adequately  
24 simulating the reactor content mass/volume and the TS, this model might bring further  
25 insight about potentially inhibitory mechanisms (i.e.  $\text{NH}_3$  buildup and/or acidification)  
26 occurring in HS-AD of OFMSW.

27

28 **Keywords:** High-Solids Anaerobic Digestion; ADM1; Reactor Mass Simulation; Total  
29 Solids; Apparent Concentrations.

30

## 31 1 INTRODUCTION

32 Anaerobic digestion (AD) is a biochemical treatment technology for organic waste  
33 valorization yielding a high-methane-content biogas and a partially stabilized organic  
34 material with potential applications as soil amendment (Mata-Alvarez 2003). High-  
35 solids anaerobic digestion (HS-AD) is a particular case of AD operated at a total solid  
36 (TS) content  $\geq 10\%$ , in contrast to 'wet' AD applications (i.e. TS  $< 10\%$ ) (Abbassi-  
37 Guendouz et al. 2012). Thus, HS-AD has the advantage of minimizing the reactor  
38 volume, as well as the need for water addition. On the other hand, HS-AD is normally  
39 associated with an important reduction of the total (TS) and volatile (VS) solid content,  
40 during the biological degradation of the organic matter. For example, HS-AD of the  
41 organic fraction of municipal solid waste (OFMSW) might lead to a TS removal of 30 -  
42 80 % (Cecchi et al. 2002, Mata-Alvarez 2003, Pavan et al. 2000). However, some  
43 drawbacks limit the applicability of HS-AD as, for example, the reduced kinetics  
44 expected as a consequence of the hampered mass transfer, and the high risk of  
45 acidification due to organic overloading (Benbelkacem et al. 2015, De Baere 2000).  
46 Among the solid wastes used in HS-AD, the OFMSW is particularly suited for  
47 anaerobic treatment due to its elevated TS content (i.e. 25 - 30 %), biodegradation  
48 potential and possibility to recover nutrients (i.e. nitrogen and phosphorous) from its  
49 composition (De Baere and Mattheeuws 2013, Mata-Alvarez 2003). However, HS-AD  
50 of OFMSW is normally associated with a high risk of inhibition due to the high protein  
51 content, leading to free ammonia nitrogen ( $\text{NH}_3$ ), as one of the most important  
52 inhibitors (Chen et al. 2008, Kayhanian 1999, Rajagopal et al. 2013).  
53 Understanding the biochemical and physicochemical dynamics in HS-AD is crucial to  
54 ease the design and operation of HS-AD reactors, minimizing the risk of

55 acidification/inhibition. Particularly important is the knowledge about the interactions  
56 between the main four phases – microorganisms, solids, liquids and gases – in HS-AD,  
57 since it might allow to increase the waste treatment capabilities and methane yield  
58 (Mata-Alvarez 2003, Vavilin et al. 2004, Xu et al. 2015). In this line, an adapted  
59 mathematical model is required for the operational analysis and technology  
60 development of HS-AD, as some of the main applications for ‘wet’ AD of the anaerobic  
61 digestion model No.1 (ADM1) (Batstone 2006, Batstone et al. 2002, Batstone et al.  
62 2015, Xu et al. 2015).

63 ADM1 is a structured model gathering together the main biochemical and  
64 physicochemical processes of AD (Batstone et al. 2002, Batstone et al. 2015).  
65 Biochemical processes include the disintegration, hydrolysis, acidogenesis, acetogenesis  
66 and methanogenesis of complex substrates composed of carbohydrates, proteins and  
67 lipids in chemical oxygen demand (COD) units. Physicochemical processes include the  
68 gas transfer and the equilibrium of the ionic species of the main inorganic compounds in  
69 AD (i.e. CO<sub>2</sub> and NH<sub>3</sub>). However, the CSTR implementation of ADM1 was primarily  
70 conceived for ‘wet’ AD applications (i.e. TS << 10 %), while a more complex  
71 hydraulic and particulate component modeling is required for HS-AD (Batstone et al.  
72 2002, Batstone et al. 2015, Xu et al. 2015). Thus, modelling HS-AD might be  
73 particularly challenging due to the intrinsic complexity of the process (Batstone et al.  
74 2015, Mata-Alvarez et al. 2000, Vavilin et al. 2004, Xu et al. 2015). For example, the  
75 (semi-)solid matrix might define the soluble/gaseous transport processes, as well as the  
76 capabilities of anaerobic biomass to access the substrates (Bollon et al. 2013, Vavilin  
77 and Angelidaki 2005).

78 The mass balance modification, regarding the continuously stirred tank reactor (CSTR)  
79 implementation of ADM1 (Batstone et al. 2002), is required to account for the reactor  
80 content mass ( $M_{Global}$ ) removal and the specific weight ( $\rho_{Global}$ ) dynamics in HS-AD  
81 (Batstone et al. 2015, Kayhanian and Hardy 1994, Richards et al. 1991, Vavilin et al.  
82 2004). Noteworthy, the reactor content volume ( $V_{Global}$ ) might describe important  
83 fluctuations during HS-AD, depending mainly on the substrate TS and biodegradability,  
84 in contrast to ‘wet’ AD. Furthermore, a given degree of gaseous porosity ( $\epsilon$ ) might be  
85 present in the HS-AD matrix, particularly at TS contents  $\geq 25$  % (Batstone et al. 2015,  
86 Benbelkacem et al. 2013, Bollon et al. 2013, Vavilin et al. 2003). ADM1 was originally  
87 expressed in volumetric units (i.e. kg COD/m<sup>3</sup>). Meanwhile, the most common  
88 measurements in HS-AD are normally expressed in mass units (i.e. kg COD/kg), since  
89 accounting for the specific weight of (semi-)solid samples – but also the specific weight  
90 dynamics in HS-AD – involves the complexity of the analytical techniques  
91 (Benbelkacem et al. 2013, Bollon et al. 2013, Kayhanian and Tchobanoglous 1996). For  
92 example, the specific weight of a (semi-)solid sample can be approximated by the use of  
93 a water pycnometer, where the sample must be appropriately pretreated (i.e.  
94 dried/ground), the distilled water fully degassed and analyses performed under  
95 temperature-controlled conditions (ASTM 2002). With all the above, HS-AD  
96 simulations need to be approached differently than in ‘wet’ AD, where  $\rho_{Global}$  and  $V_{Global}$   
97 are normally assumed constant, as summarized in Figure 1.

98 This study aimed at developing a mathematical tool based on the ADM1 biochemical  
99 framework, capable of simulating the solids and reactor content mass/volume dynamics  
100 in HS-AD of OFMSW, including the interrelationship between TS (and VS) removal  
101 and biogas production. By simulating adequately the global mass/volume and TS

102 dynamics, the presented model might serve as a link between ‘wet’ AD and HS-AD,  
103 while it might help to explore potential inhibitory/acidification mechanisms occurring  
104 during HS-AD of OFMSW. Meanwhile, the proposed model was aimed to be as general  
105 as possible, since different HS-AD applications (i.e. organic substrate and/or reactor  
106 configuration) could be simulated, provided that the main hypotheses presented in the  
107 methodology section are fulfilled. Furthermore, the eventual model user is encouraged  
108 to further calibrate the model parameters and/or modify the model structure, in order to  
109 adapt the HS-AD model for any specific need.

110

## 111 **2 MATERIALS AND METHODS**

### 112 **2.1 High-Solids Model Implementation**

113 The main basis for the dynamic model presented in this study was ADM1 (Batstone et  
114 al. 2002), including the modifications suggested by Blumensaat and Keller (2005) for  
115 closing nitrogen and carbon balances. The simulation of the HS-AD of OFMSW  
116 required four preliminary hypotheses in order to reduce the complexity of the model.  
117 Firstly, HS-AD was assumed to take place in a homogenized (i.e. completely mixed)  
118 reactor [Hypothesis 1]. Secondly, the effect of porosity and transport processes was  
119 assumed to be negligible [Hypothesis 2]. Then, the specific weight of solids and solvent  
120 was considered constant [Hypothesis 3]. Finally, the biochemical reactions were  
121 assumed to occur predominantly in water [Hypothesis 4].

122 With these hypotheses, ADM1 required some particular modifications in order to  
123 simulate the TS and mass/volume dynamics in HS-AD, while allowing the calibration  
124 of the proposed model. The main modifications implemented in ADM1 in order to  
125 simulate HS-AD were the inclusion of mass balances modifying the reactor mass and



126 volume (needed to account for the organic solid removal in HS-AD) and the inclusion  
 127 of apparent concentrations (as a link between ‘wet’ and high-solids applications).

128

### 129 **2.1.1 Mass Balances in High-Solid Anaerobic Digestion Reactors**

130 The simulation of the reactor mass and TS/VS content of homogenized HS-AD reactors  
 131 required the implementation of the global ( $M_{Global}$ ) [Equation 1], solid material ( $M_{Solids}$ )  
 132 [Equation 2], liquid-solvent content ( $M_{Solvent}$ ) [Equation 3] and inert material ( $M_{Inerts}$ )  
 133 [Equation 4] mass balances. In this study, the solvent was considered as only water,  
 134 while the solid material included all the organic and inorganic compounds (i.e.  
 135 particulates and soluble compounds, VFA, microorganisms) inside the reactor, except  
 136 water. In mass balances, the mass content ( $M_i$ ) – global or partial – dynamics were  
 137 related to the corresponding mass fluxes ( $m_i$ ), particularly the gases flowing out of the  
 138 reactor as a consequence of methanogenesis. The implementation of reactor mass  
 139 balances is crucial in HS-AD, since it accounts for the importance of mass and water  
 140 removal due to biogas production, in contrast to ‘wet’ AD (Henze et al. 1997,  
 141 Kayhanian and Tchobanoglous 1996, Richards et al. 1991).

$$\frac{dM_{Global}}{dt} = m_{Influent,Global} - m_{Effluent,Global} - m_{Biogas} \quad (1)$$

$$\frac{dM_{Solids}}{dt} = m_{Influent,Solids} - m_{Effluent,Solids} - (m_{Biogas} - m_{Vapor}) \quad (2)$$

$$\frac{dM_{Solvent}}{dt} = m_{Influent,Solvent} - m_{Effluent,Solvent} - m_{Vapor} \quad (3)$$

$$\frac{dM_{Inerts}}{dt} = m_{Influent,Inerts} - m_{Effluent,Inerts} \quad (4)$$

142

143 The biogas ( $m_{Biogas}$ ) [Equation 5] and vapor ( $m_{Vapor}$ ) [Equation 6] outflows in the mass  
 144 balances were calculated from the volumetric biogas flow ( $Q_g$ ), obtained as shown in

145 the CSTR implementation of ADM1 (Batstone et al. 2002), by using the molar gas  
 146 composition ( $x_i$ ) and the molecular weight ( $Mr_i$ ) of each gaseous compound in the gas  
 147 phase. The biogas was assumed to be composed of CH<sub>4</sub>, CO<sub>2</sub>, H<sub>2</sub>, H<sub>2</sub>O and NH<sub>3</sub>. The  
 148 reactor headspace was assumed to be vapor saturated, being vapor pressure ( $P_v$ )  
 149 expressed as a function of temperature (T). On the other hand, an inert gas was added to  
 150 account for the initial flushing in AD experiments (i.e. by N<sub>2</sub>), assuming for it a  
 151 negligible liquid solubility. Importantly, the inert gas was not included in  $m_{Biogas}$   
 152 calculations. Once knowing the  $M_{Global}$ ,  $M_{Solids}$  and  $M_{Inerts}$ , the TS and VS contents were  
 153 approximated in dynamic mode by using the corresponding definition (EPA 2001)  
 154 [Equations 7 & 8]. Noteworthy, TS and VS in the proposed model were dimensionless  
 155 (i.e. kg Solids/kg Total), varying from 0 to 1.

$$m_{Biogas} = \frac{P_T Q_g}{RT} \sum x_i Mr_i \quad (5)$$

$$m_{Vapor} = \frac{P_v Q_g}{RT} Mr_{H2O} \quad (6)$$

$$TS = \frac{M_{Solids}}{M_{Global}} \quad (7)$$

$$VS = \frac{M_{Solids} - M_{Inerts}}{M_{Global}} \quad (8)$$

156  
 157 The liquid-gas transfer of gaseous species in the CSTR implementation of ADM1  
 158 depends on the ratio between the reactor content volume ( $V_{Global}$ ; 'V<sub>liq</sub>' in ADM1) and  
 159 the gas volume ( $V_g$ ), while their sum yields the design/overall reactor volume ( $V_{Reactor}$ )  
 160 (Batstone et al. 2002). Thus, since a considerable reduction of  $V_{Global}$  – alongside  $M_{Global}$   
 161 removal – can occur in HS-AD associated with methanogenesis, the reactor volume was  
 162 approximated by the specific weigh of the reactor content ( $\rho_{Global}$ ). Importantly,  $\rho_{Global}$   
 163 varies also in HS-AD, as it gathers together the individual dynamics of all the mass

164 compounds in the system (Kayhanian and Tchobanoglous 1996). Therefore, to simulate  
 165  $\rho_{Global}$ , it is necessary to know the specific weight of all the materials within HS-AD ( $\rho_i$ ),  
 166 but also their corresponding mass fraction ( $m_i$ ) [Equation 9]. For simplicity, the  
 167 simulations in this study used a common specific weight for all the solid compounds  
 168 ( $\rho_{Solids}$ ) and a solvent specific weight ( $\rho_{Solvent}$ ). With these simplifications, the  $V_{Global}$   
 169 dynamics could be approximated with Equation 10.

$$\frac{1}{\rho_{Global}} = \sum_i \frac{m_i}{\rho_i} \quad (9)$$

$$\frac{dV_{Global}}{dt} = \frac{1}{\rho_{Solids}} \cdot \frac{dM_{Solids}}{dt} + \frac{1}{\rho_{Solvent}} \cdot \frac{dM_{Solvent}}{dt} \quad (10)$$

170  
 171 The distinction between mass and volume in the proposed model for homogenized HS-  
 172 AD reactors permitted the use of ADM1 volumetric units (i.e. kmol/m<sup>3</sup>), while  
 173 implementing the different influent and effluent mass and/or volumetric flows when  
 174 operating HS-AD in (semi-)continuous mode. Finally, for illustrative purposes only, an  
 175 adaptive volumetric effluent ( $Q_{Effluent}$ ) was added to the model – in terms of a  
 176 proportional controller – to maintain  $V_{Global}$  if required. This strategy permitted to  
 177 compensate for the potential organic mass removal in HS-AD and, therefore, to stabilize  
 178 the HS-AD system, as further discussed in section 3.1. A schematic diagram of the HS-  
 179 AD model implementation for homogenized reactors is shown in Figure 2.

180

### 181 **2.1.2 Apparent Concentrations – Soluble Species Recalculation**

182 The (soluble) apparent concentrations ( $S_{T,i,App}$ ) were used in the HS-AD model  
 183 biochemistry and physicochemistry to reproduce the effect of high TS in HS-AD, in  
 184 contrast to ‘wet’ AD. This modification was related to the assumption that the main  
 185 biochemical reactions might occur predominantly in the presence of water (Hypothesis

186 4). Similarly, the apparent concentrations served to link the global (i.e. kmol/kg Total)  
 187 and liquid fraction (i.e. kmol/kg Solvent) measurements in HS-AD. The apparent  
 188 concentrations were calculated for all the soluble species of ADM1 using TS,  $\rho_{Global}$  and  
 189  $\rho_{Solvent}$  [Equation 11]. Importantly, the long chain fatty acids (LCFA,  $S_{fa}$ ) were not  
 190 considered as soluble in HS-AD, due to their highly non-polar nature and reduced  
 191 solubility in water (i.e. palmitic acid solubility = 1.2 mg/L at 60 °C). With this approach,  
 192 the proposed model simulates the mass balance of dynamic variables ( $C_{T,i}$ ) – either  
 193 particulate ( $X_{T,i}$ ) or soluble ( $S_{T,i}$ ) – as a function of  $V_{Global}$  (i.e. kmol/m<sup>3</sup> Total)  
 194 [Equation 12], while the apparent concentrations ( $S_{T,i,App}$ ) (i.e. kmol/m<sup>3</sup> Solvent) were  
 195 used only for the soluble species included in the biochemical and physicochemical rates  
 196 of ADM1 ( $r_{i,ADM1}$ ) (i.e. uptake of acetate). It is important to mention that Equation 12 is  
 197 the mass balance of an individual component in AD and, therefore, should be based in  
 198 the chain rule in order to account for the  $V_{Global}$  dynamics, in contrast to the CSTR  
 199 implementation of ADM1 (Batstone et al. 2002). On the other hand, it should be noted  
 200 that the effect of apparent concentrations becomes negligible at low TS contents (i.e. TS  
 201 < 5 %) with  $\rho_{Global}$  tending to  $\rho_{Solvent}$ , as  $S_{T,i,App}$  progressively approaches to  $S_{T,i}$  in these  
 202 conditions. With all the above, the sole implementation of the HS-AD mass balances  
 203 and the use of apparent concentrations in this study might allow to simulate indistinctly  
 204 ‘wet’ AD and HS-AD conditions, and/or the transition between these two AD regimes,  
 205 for example, during a prolonged HS-AD operation.

$$S_{T,i,App} \left( \frac{kg \text{ or } kmol}{m^3 \text{ Solvent}} \right) = \frac{S_{T,i} \left( \frac{kg \text{ COD or } kmol}{m^3 \text{ Total}} \right)}{(1 - TS) \left( \frac{kg \text{ Solvent}}{kg \text{ Total}} \right)} \cdot \frac{\rho_{Solvent} \left( \frac{kg \text{ Solvent}}{m^3 \text{ Solvent}} \right)}{\rho_{Global} \left( \frac{kg \text{ Total}}{m^3 \text{ Total}} \right)} \quad (11)$$

$$\frac{dC_{T,i}}{dt} = \frac{1}{V_{Global}} \cdot \left( Q_{Influent} \cdot C_{T,0} - \frac{m_{Effluent}}{\rho_{Global}} \cdot C_{T,i} \right) + \sum r_{i,ADM1} - \frac{C_{T,i}}{V_{Global}} \cdot \frac{dV_{Global}}{dt} \quad (12)$$

206

207 **2.1.3 Kinetic Rates**

208 The ADM1 biochemical rates and inhibitions were used for the verification of the  
 209 model implementation according to the protocol proposed by Rosén and Jeppsson  
 210 (2006). The model verification aimed to test/assess the ADM1 implementation (code)  
 211 alongside the adequate mathematical solution of the mass balances, determining the TS  
 212 and organic removal both in ‘wet’ and high-solids AD applications. On the other hand,  
 213 a slightly different set of biochemical rates was used for HS-AD model calibration.  
 214 Thus, calibration aimed to test/assess the HS-AD model performance under real  
 215 experimental conditions. The biochemical kinetics used in this study are shown in Table  
 216 1.

217 The biochemical rates used in the HS-AD model were associated with the inhibitory  
 218 functions as originally proposed in ADM1 (Batstone et al. 2002, Rosén and Jeppsson  
 219 2006) [Equations 13 to 16]. However, all the soluble species terms included in the HS-  
 220 AD biochemical rates – excluding  $S_{fa}$  – were expressed in terms of apparent  
 221 concentrations, as mentioned in section 2.1.2.

$$I_{in} = \frac{S_{in,App}}{K_{S,Sin} + S_{in,App}} \quad (13)$$

$$I_{h2} = \frac{K_{i,Sh2}}{K_{i,Sh2} + S_{h2,App}} \quad (14)$$

$$I_{pH} = \frac{K_{pH}^{N_{pH}}}{K_{pH}^{N_{pH}} + S_{proton}^{N_{pH}}} \quad (15)$$

$$I_{nh3} = \frac{K_{i,Shh3}}{K_{i,Shh3} + S_{nh3,App}} \quad (16)$$

222  
223 Regarding the HS-AD model implementation used for calibration [Table 1], the valerate  
224 uptake was assumed to be carried out by valerate degraders ( $X_{c5}$ ), instead of butyrate  
225 and valerate being both degraded by butyrate degraders ( $X_{c4}$ ), as proposed in ADM1  
226 (Batstone et al. 2002). This last modification was used to account for the different  
227 dynamics observed for butyrate and valerate uptake in the experimental data. The  
228 valerate parameters and rates were maintained as in the original thermophilic (55 °C)  
229 implementation of ADM1, though the  $X_{c5}$  decay was included in the biochemical  
230 matrix. On the other hand, the microbial decay was assumed to yield particulate  
231 substances (i.e. carbohydrates and proteins) directly, avoiding the use of a composite  
232 material ( $X_c$ ) and the associated disintegration kinetics (Batstone et al. 2015). The  
233 biomass decay COD fractioning (i.e.  $f_{ch,xc}$ ) was maintained as proposed by Rosén and  
234 Jeppsson (2006). However, the inert materials (i.e.  $S_i$  and  $X_i$ ) carbon content ( $C_i$ ) was  
235 modified to 0.0405 kmol C/kg COD in order to close the biomass carbon balance, while  
236 the inert nitrogen content ( $N_i$ ) was modified to 0.0144 kmol N/kg COD to close the  
237 biomass nitrogen balance. This last modification permitted to reduce the stiffness and  
238 speed up the model simulations in this study.

239 The degradation of the protein content of an organic waste determines the total  
240 ammonia nitrogen (TAN,  $S_{in}$ ) in HS-AD (Kayhanian 1999). In this line, the nitrogen  
241 balance has to be closed for the microorganisms in ADM1, while adding complex  
242 substrates implies the fulfilment of the corresponding nitrogen balances. For this study,  
243 two nitrogen balances were used for the biomass and substrate as shown in Equations  
244 17 and 18, respectively, assuming a common nitrogen content for proteins/amino acids  
245 ( $N_{aa}$ ). With this approach, two new inert variables ( $S_{i,subs}$  and  $X_{i,subs}$ ) were added to

246 ADM1 in order to calibrate the initial protein content ( $X_{pr}$ ) and/or the experimental  
 247 TAN dynamics. The nitrogen balance for biomass [Equation 17] remained closed as  
 248 mentioned before, while the protein fraction of the substrate-inoculum mixture ( $f_{pr,subs}$ )  
 249 could be adjusted by calibrating the inert nitrogen content of the substrate-inoculum  
 250 mixture ( $N_{i,subs}$ ), since all the remaining variables in the nitrogen balance ( $N_{subs}$ ,  $f_{si,subs}$   
 251 and  $f_{xi,subs}$ ) [Equation 18] could be obtained experimentally. For example, the anaerobic  
 252 biodegradability (i.e.  $COD_{removed}/COD_{substrate}$ ) of an organic substrate is equivalent to 1 -  
 253 ( $f_{si,subs} + f_{xi,subs}$ ), while the global nitrogen content of the substrate-inoculum mixture  
 254 ( $N_{subs}$ ) is the quotient between the total Kjeldahl nitrogen (TKN) and COD (i.e.  
 255  $TKN_{substrate}/COD_{substrate}$ ).

$$N_{bac} = f_{pr,xc} \cdot N_{aa} + (f_{si,xc} + f_{xi,xc}) \cdot N_i \quad (17)$$

$$N_{subs} = f_{pr,subs} \cdot N_{aa} + (f_{si,subs} + f_{xi,subs}) \cdot N_{i,subs} \quad (18)$$

256

## 257 2.2 Verification of the Model Implementation

258 The proposed model implementation was verified for ‘wet’ AD according to Rosén and  
 259 Jeppsson (2006). Similarly, the model was further tested for HS-AD conditions. In total,  
 260 four different verification scenarios were simulated: A) ‘wet’ AD using the ADM1  
 261 implementation of Rosén and Jeppsson (2006); B) ‘wet’ AD using the HS-AD model  
 262 implementation with a constant  $Q_{Effluent}$ ; C) HS-AD using the HS-AD model and  
 263 constant  $Q_{Effluent}$ ; and D) HS-AD considering the HS-AD model with an adaptive  
 264  $Q_{Effluent}$ . The HS-AD model was coded in MATLAB<sup>®</sup> R2017a. The equation resolution  
 265 was the ode15s; a variable-step, variable-order solver based on the numerical  
 266 differentiation formulas of orders 1 to 5. The influent conditions used for model  
 267 verification are shown in Table 2.

268 Noteworthy, the only difference between the influent conditions during simulations A  
269 and B was the introduction of the TS, VS and  $\rho_{\text{Global}}$  of the substrate in the last case  
270 [Table 2], permitting to excite the high-solids module of the proposed HS-AD model, in  
271 contrast to the CSTR implementation of ADM1. On the other hand, for illustrative  
272 purposes only, a high-solids substrate was included using a different carbohydrate ( $X_{\text{ch}}$ )  
273 and particulate inert ( $X_{\text{i}}$ ) content, but also TS, VS and  $\rho_{\text{Global}}$ , for simulations C and D  
274 [Table 2]. Thus, the high TS content of the influent conditions (i.e. 25 %), associated  
275 predominantly with  $X_{\text{ch}}$  and  $X_{\text{i}}$ , permitted to test the model under HS-AD operation,  
276 while avoiding potential inhibitory states due to  $\text{NH}_3$  accumulation.

277 During the verification of the model implementation, all the ADM1 parameters were  
278 used as proposed by Rosén and Jeppsson (2006) for mesophilic (35 °C) AD operation,  
279 though the original hydrolysis constant for carbohydrates ( $k_{\text{h,ch}}$ ) had to be reduced to  
280 0.10 days in the HS-AD verification only (simulations C and D), in order to avoid  
281 reactor overloading and acidification (i.e.  $\text{pH} \leq 6.0$ ) during the initial days of  
282 simulation. 200 days of ‘wet’ AD or HS-AD operation were simulated for each  
283 verification scenario. The organic loading rate (OLR) was evaluated as the daily  
284 substrate addition in COD units divided by  $V_{\text{Global}}$ , while the hydraulic retention time  
285 (HRT) was evaluated as the quotient between  $V_{\text{Global}}$  and  $Q_{\text{Effluent}}$ .

286

### 287 **2.3 Experimental Data and Data Recalculation**

288 The experimental data used to calibrate the HS-AD model consisted in a batch-sacrifice  
289 test fed with dried OFMSW and centrifuged inoculum at TS of 15 % operated under  
290 thermophilic (55 °C) conditions. In the sacrifice test, 15 replicates were implemented in  
291 250 mL serum bottles. Thus, after measuring the biogas volume and composition, a



292 single replicate was opened, and the HS-AD content thoroughly analyzed for the main  
 293 physicochemical variables. The experimental results included the TS, VS,  $\rho_{Global}$ , COD,  
 294 TKN, TAN, pH, volatile fatty acids (VFA; valeric, butyric, propionic and acetic acids),  
 295 mono-valent ions ( $Na^+$ ,  $K^+$  and  $Cl^-$ ), biogas composition ( $CH_4$ ,  $CO_2$  and  $H_2$ ) and  
 296 methane yield. The serum bottles were agitated only on those days when the biogas  
 297 production was measured. Further information about the experimental setup, substrate,  
 298 inoculum and physicochemical analyses is presented as Supplementary Information.  
 299 Importantly, an experimental bias might exist on TS measurements whether volatile  
 300 compounds (i.e.  $NH_3$ ,  $CO_2$  and VFA) are lost when drying at 105 °C (Angelidaki et al.  
 301 2009, EPA 2001). For this study, the mass of volatile substances at 105 °C ( $M_{Volatiles}$ )  
 302 was assumed to be equivalent to the total mass of VFA ( $S_{ac}$ ,  $S_{pro}$ ,  $S_{bu}$  and  $S_{va}$ ), TAN ( $S_{in}$ )  
 303 and inorganic carbon ( $S_{ic}$ ) [Equation 19]. Thus, the simulated TS and VS were  
 304 recalculated *a posteriori* ( $TS_{Recalc}$  and  $VS_{Recalc}$ ) [Equation 20 and 21] in order to  
 305 compare them with the experimental values.

$$M_{Volatiles} = (S_{ac} \cdot \frac{60}{64} + S_{pro} \cdot \frac{74}{112} + S_{bu} \cdot \frac{88}{160} + S_{va} \cdot \frac{102}{208} + S_{in} \cdot 17 + S_{ic} \cdot 44) \cdot V_{Global} \quad (19)$$

$$TS_{Recalc} = \frac{M_{Solids} - M_{Volatiles}}{M_{Global}} \quad (20)$$

$$VS_{Recalc} = \frac{M_{Solids} - M_{Inerts} - M_{Volatiles}}{M_{Global}} \quad (21)$$

306

## 307 2.4 Model Calibration

308 The calibration of some of the main biochemical parameters in this study aimed to  
 309 obtain the best fitting with the experimental data for a homogenized HS-AD laboratory-  
 310 scale reactor, in order to assess the correct simulations of the TS and reactor content  
 311 dynamics. The model calibration was carried out by trial and error, mainly for the

312 hydrolysis (i.e.  $k_{h,ch}$ ) and maximum growth rate (i.e.  $k_{m,su}$ ) constants, aiming to maintain  
313 as close as possible the parameters proposed for thermophilic (55 °C) AD in ADM1  
314 (Batstone et al. 2002). Noteworthy, the initial composition (i.e.  $S_{ac}$ ,  $S_{in}$ ) was chosen  
315 based on the evaluation of the experimental data available (i.e. VFA, TAN), while all  
316 the initial microorganisms concentrations (i.e.  $X_{ac}$ ,  $X_{su}$ ) were calibrated also by trial and  
317 error, alongside the main biochemical parameters, as further discussed in section 3.2.1.

318

### 319 **3 RESULTS AND DISCUSSION**

#### 320 **3.1 Model Implementation Verification**

##### 321 **3.1.1 'Wet' AD Verification**

322 The model verification for 'wet' AD operating in a CSTR (simulation A) showed  
323 minimal differences (i.e. 4<sup>th</sup>-5<sup>th</sup> significant digit) compared to the results suggested by  
324 Rosén and Jeppsson (2006) [Table 3], being these differences likely associated with the  
325 slightly different equation resolution method used [U. Jeppsson, Personal  
326 Communication]. Importantly, when using the HS-AD model implementation for 'wet'  
327 AD (simulation B), the results were again very close to the original 'wet' ADM1  
328 verification, though some differences could be observed for all the dynamic variables  
329 [Table 3]. For example, the acetic acid ( $S_{ac}$ ) predicted with the HS-AD model  
330 implementation (simulation B) was around 39 % higher than that in the original ADM1  
331 (simulation A). The TS concentration effect of apparent concentrations might define  
332 some differences among all the soluble species during 'wet' AD (i.e.  $S_{ac}$ ,  $S_{h2}$ ,  $S_{nh3}$ ),  
333 though the apparent concentrations effect in 'wet' applications was relatively small in  
334 simulation B due to the low TS content (i.e. < 5 %) [Equation 11].

335 It is important to mention that the differences between simulations A and B were related  
336 to the fact that the ‘wet’ AD simulation using the HS-AD model (simulation B) did not  
337 reach steady-state. Thus, a steady-state operation in simulation B was not reached even  
338 after 200 days, particularly due to the implementation of a common volumetric  
339 influent/effluent (i.e.  $Q_{\text{Influent}} = Q_{\text{Effluent}}$ ). In this line, simulation B showed an overall  
340 37 % reduction in the TS content after 200 days, as well as a 13 % reduction in the  
341  $V_{\text{Global}}$  (but also HRT), and a 0.5 % reduction in  $\rho_{\text{Global}}$  [Table 3]. Therefore, a daily-  
342 averaged 0.06 %  $V_{\text{Global}}$  modification occurred in ‘wet’ AD using the HS-AD model,  
343 which might be considered negligible for short operation periods, but increasingly  
344 important for longer operation (Henze et al. 1997, Richards et al. 1991). The  
345 progressive reduction of the HRT during simulation B led to a proportional increase in  
346 the OLR from 2.85 to 3.27 kg COD/m<sup>3</sup>·d [Figure 3a], explaining the differences  
347 between simulations A and B (i.e.  $S_{\text{ac}}$ ) mentioned before. Interestingly, the reduction in  
348  $\rho_{\text{Global}}$  (i.e. 0.994 kg/L) below  $\rho_{\text{Solvent}}$  (i.e. 1.000 kg/L) suggests that the influent  
349 conditions (i.e.  $\rho_{\text{Global}0} = \rho_{\text{Solvent}}$ ) and/or the model simplifications (i.e.  $\rho_{\text{Solids}} = \text{const.}$ )  
350 required further testing.

351 The specific weight of a complex sample ( $\rho_{\text{Global}}$ ) depends on all the compounds  
352 involved [Equation 9]. Since the measurement of all the variables  $\rho_i$  in an AD sample is  
353 rarely available, the  $\rho_i$  of each compound needs to be known/assumed for simulations.  
354 In this line, the specific weight of a sample solid fraction ( $\rho_{\text{Solids}}$ ) can be approximated  
355 by knowing the specific weight of the solvent ( $\rho_{\text{Solvent}}$ ), though  $\rho_{\text{Solvent}}$  is again function  
356 of all the different compounds in solution, as well as a function of temperature and  
357 pressure (Lide 2004). As a preliminary approach,  $\rho_{\text{Solvent}}$  was assumed to be close to the  
358 specific weight (density) of water at 0 °C and 1 bar (i.e.  $\rho_{\text{Solvent}} = 1 \text{ kg/L}$ ), since the

359 density of water is  $999.84 \text{ kg/m}^3$  at  $0 \text{ }^\circ\text{C}$ ,  $993.64 \text{ kg/m}^3$  (0.63 % error) at  $35 \text{ }^\circ\text{C}$ , and  
360  $985.19 \text{ kg/m}^3$  (1.48 % error) at  $55 \text{ }^\circ\text{C}$  (Kell 1975, Lide 2004), thus being approximately  
361 constant at any of these temperatures. With this strategy, the specific weights obtained  
362 for the overall sample ( $\rho_{\text{Global}}$ ) and/or the solid fraction ( $\rho_{\text{Solids}}$ ) were considered relative  
363 regarding the specific weight of solvent ( $\rho_{\text{Solvent}}$ ). Meanwhile,  $\rho_{\text{Solvent}}$  (but also  $\rho_{\text{Solids}}$ )  
364 could be set to any value, or modified by any expression (i.e. as a function of  
365 temperature), without modifying the structure of the model. Thus, once knowing the  
366  $\rho_{\text{Solvent}}$ , the  $\rho_{\text{Global}}$  and TS of a (semi-)solid sample,  $\rho_{\text{Solids}}$  could be approximated by  
367 using the mass balance [Equation 9].

368 Previous research indicated that  $\rho_{\text{Solids}}$  ranges from  $1.3 \text{ kg/L}$  in lignocellulosic materials  
369 to  $1.5 \text{ kg/L}$  in OFMSW and  $2.5 \text{ kg/L}$  for inorganic inert solids (i.e. sand). On the other  
370 hand, the specific weight of microorganisms is reported between  $0.8$  and  $1.4 \text{ kg/L}$  (van  
371 Veen and Paul 1979), though this fraction might be a negligible part (i.e. 5 %) of the  
372 whole reactor mass content. Therefore, a compromise value of  $\rho_{\text{Solids}} = 1.5 \text{ kg/L}$  was  
373 chosen for the preliminary model verification/calibration, though further testing must be  
374 devoted to this particular variable, since it could influence other aspects of the HS-AD  
375 simulations (i.e.  $V_{\text{Global}}$ ), as mentioned before.

376

### 377 **3.1.2 HS-AD Verification**

378 Regarding the HS-AD model verification with constant  $Q_{\text{Effluent}}$  (simulation C), the HS-  
379 AD simulation did not reach the steady state after 200 days, while longer simulations  
380 (i.e. 365 days) yielded reactor acidification (i.e.  $\text{pH} \leq 6.0$ ) – data not shown. This is due  
381 to a progressive reduction of  $V_{\text{Global}}$  in HS-AD when maintaining a volumetric outflow  
382 equal to the volumetric inflow (i.e.  $Q_{\text{Influent}} = Q_{\text{Effluent}}$ ) (Kayhanian and Tchobanoglous

1996, Richards et al. 1991). Thus, the HRT decreases – and the OLR increases –  
proportionally to the  $V_{\text{Global}}$  reduction in HS-AD until the ‘washout’ of methanogens  
occurs and the reactor acidifies. For example, a 50 % reduction in HRT was observed  
with the influent conditions tested in simulation C [Figure 3b], with an approximately  
daily-averaged  $V_{\text{Global}}$  reduction of 0.25 %.

Meanwhile, a rapid stabilization of the HS-AD process was obtained when choosing a  
constant reactor volume as a set point (i.e.  $V_{\text{Setpoint}} = V_{\text{Global0}}$ ) and recalculating  $Q_{\text{Effluent}}$   
[Table 3 and Figure 3b]. Noteworthy, the  $Q_{\text{Effluent}}$  recalculation operation yielded a  
reduction of around 5.6 % of the steady-state value regarding  $Q_{\text{Influent}}$ , and a 24 % TS  
removal compared to the substrate TS (i.e. from 25 to 19 %). These results condense the  
importance of reducing the effluent compared to the influent (i.e.  $Q_{\text{Influent}} > Q_{\text{Effluent}}$ ) to  
reach steady-state HS-AD, in order to compensate the organic removal by  
methanogenesis (Kayhanian and Hardy 1994, Kayhanian and Tchobanoglous 1996,  
Richards et al. 1991). Furthermore, the use of apparent concentrations might be also  
crucial for HS-AD simulations, since practically all the biochemical rates were affected  
(i.e. speeded-up/slowed-down) by the TS concentration effect on soluble substrates (i.e.  
 $S_{\text{ac}}$ ) and/or inhibitors (i.e.  $S_{\text{nh}_3}$ ) [Table 1]. For example, a 26 % increase in all the  
soluble concentrations (i.e.  $S_{\text{su}}$  and  $S_{\text{h}_2}$ ) was obtained by the tested HS-AD conditions in  
steady-state operation – data not shown.

The water/solvent in this study was assumed to be conservative, since the same water  
entering leaves the system as a liquid effluent ( $m_{\text{Effluent,Solvent}}$ ) or vapor ( $m_{\text{vapor}}$ ), but is  
not produced/consumed. Importantly, production/consumption of water in the  
biochemical processes (i.e. hydrolysis, methanogenesis) might occur, linking Equations  
2 and 3. However, the production/consumption of water is tightly linked to the

407 stoichiometry of all the reactions occurring in HS-AD, while the stoichiometry of all the  
408 biochemical reactions in ADM1 requires further development (De Gracia et al. 2006,  
409 Kleerebezem and van Loosdrecht 2006, Rodríguez et al. 2006). Therefore, using  
410 Equations 1 to 4 is a reasonable hypothesis that can be modified, once the global  
411 stoichiometry of HS-AD is well-defined. In this last case, the Petersen matrix originally  
412 proposed for ADM1 would need to account for water as another dynamic variable. For  
413 example, De Gracia et al. (2006) included water (i.e.  $S_{H_2O}$ ) in the Petersen matrix of  
414 ADM1, though the AD stoichiometry was partially assumed (i.e. elemental  
415 composition). Furthermore, in order to use Equations 1 to 4 in this study, it was also  
416 assumed that the organic solid destruction only proceeds when biogas production  
417 occurs. In other words, whether hydrolysis, acidogenesis and/or acetogenesis occur, but  
418 not biogas production (i.e.  $CH_4$ ,  $CO_2$  and/or  $H_2$ ), complex substrates (i.e. carbohydrates)  
419 are just transformed into more simple substrates (i.e. sugars, VFA), being both of them  
420 jointly included in the term  $m_{Effluent, Solids}$ . With these two last assumptions, the  
421 hydrolysis to acidogenesis steps were not included in Equations 1 to 4. However, the  
422 mass volatile compounds at 105 °C ( $M_{Volatiles}$ ) needed to be accounted in the TS and VS  
423 calculations, as shown in Equations 19 to 21.

424 Due to the considerably higher COD of the influent conditions [Table 2], the OLR was  
425 around 7 times higher for HS-AD than for 'wet' AD simulations [Table 3], which  
426 directly relates to the higher chances of HS-AD acidification, and the necessity to  
427 reduce considerably the  $k_{h, ch}$  for HS-AD simulations. In either case, HS-AD  
428 experimental data are required to calibrate biochemical parameters (i.e.  $k_{h, ch}$ ).

429

### 430 **3.2 Model Calibration**

### 431 3.2.1 Comparison Between Simulated and Experimental Values

432 The HS-AD simulation of OFMSW in batch conditions at 15 % TS closely matched all  
433 the experimental variables [Figure 4], though slight disagreements were also observed  
434 between the experimental data and the simulated values. The initial conditions and  
435 modified parameters used are shown in Tables 2 and 4, respectively. Firstly, the  
436 cumulative methane production was 830 NmL CH<sub>4</sub> [Figure 4a], coinciding to that  
437 obtained experimentally, while the biogas composition was also well simulated – data  
438 not shown. Importantly, the overall biogas production was associated with 1.7 g M<sub>Global</sub>  
439 removal (i.e. 4.6 %), in agreement with the 1.5 - 2.0 g that could have been removed  
440 according to the experimental biogas flow/composition. Noteworthy, the simulation  
441 suggested that  $\rho_{Global}$  was reduced from 1078 to 1064 kg/m<sup>3</sup> (i.e. 1.2 % reduction) along  
442 the whole experimental period (data not shown), though the  $\rho_{Global}$  modification should  
443 be further validated with experimental data, as discussed before. The M<sub>Global</sub> and  $\rho_{Global}$   
444 modification yielded a V<sub>Global</sub> reduction of 3.5 % – data not shown.

445 The initial composition in the batch experiment [Table 2] was based on the availability  
446 of experimental data (i.e. COD, TS and CH<sub>4</sub> yield), but also on a reasoned assessment  
447 of the substrate and/or inoculum composition. For example, the protein content of the  
448 substrate/inoculum mixture (i.e. X<sub>pr</sub> + S<sub>aa</sub>) was adjusted according to the nitrogen  
449 content of proteins and amino acids (N<sub>aa</sub>) [Table 4] and the inert materials (i.e. X<sub>i</sub> + S<sub>i</sub>)  
450 to simulate the TAN (S<sub>in</sub>) dynamics, as mentioned in section 2.1.3. Unfortunately, apart  
451 from the CH<sub>4</sub> yield and COD of the initial mixture, no data were available regarding the  
452 remaining complex substances (i.e. particulates) involved in the biochemical framework  
453 of the model. Therefore, the distinction between the initial carbohydrate/sugars (X<sub>ch</sub>/S<sub>su</sub>)

454 and lipids/LCFA ( $X_g/S_{fa}$ ) had to be tuned alongside the biochemical parameters to  
455 simulate the initial days of the batch setup.

456 During the initial 20 days of experiment, pH was observed to drop from 7.3 to 6.3 –  
457 data not shown – due to VFA accumulation [Figure 4b]. Thus, the initial VFA and pH  
458 dynamics were simulated by a plausible set of microorganism concentrations,  
459 hydrolysis constants and initial substrate/inoculum fractionation [Tables 2 and 4]. The  
460 initial microbial concentrations are crucial in the simulation of AD batch experiments,  
461 though they are normally unknown due to the difficulties for measuring the populations  
462 involved (Donoso-Bravo et al. 2011, Flotats et al. 2010). Importantly, the hydrolysis  
463 constants ( $k_h$ ) were considerably reduced compared to the original values proposed in  
464 ADM1 for thermophilic (55 °C) operation (i.e.  $k_{h,ch} = 0.05 \text{ d}^{-1}$  vs.  $10 \text{ d}^{-1}$ , respectively),  
465 though the calibrated values were in accordance with reported hydrolysis rates for  
466 simulation of OFMSW (Batstone et al. 2002, Kayhanian 1995, Mata-Alvarez 2003,  
467 Vavilin and Angelidaki 2005).

468 In order to obtain the best fitting between the simulated and experimental VFA  
469 dynamics from day 20, the maximum growth rate ( $k_m$ ) of some microbial populations  
470 was also considerably reduced. For example, the maximum growth rate of propionate  
471 degraders ( $k_{m,pro}$ ) was reduced to  $1 \text{ d}^{-1}$ , in contrast to the  $20 \text{ d}^{-1}$  proposed by ADM1 for  
472 thermophilic (55 °C) operation [Table 4]. Noteworthy, the extremely low  $k_m$  used for  
473 model calibration, in contrast to the original values of ADM1, might be suggesting that  
474 some inhibition in the VFA uptake was occurring in the experiment. Thus,  $\text{NH}_3$  reached  
475 particularly high contents in the reactor (i.e.  $0.16 \text{ mol N/kg}$ ) [Figure 4c] mainly due to  
476 the high pH observed (i.e.  $\geq 8.0$ ), while  $\text{NH}_3$  is a well-known inhibitor of acetoclastic  
477 and hydrogenotrophic methanogens (Angelidaki and Ahring 1993, Gallert and Winter



1997, Jokela and Rintala 2003). In this line, the implementation of reversible  $\text{NH}_3$  inhibition [Equation 16] in hydrogen uptake could match adequately all the VFA, since valerate and propionate degraders are inhibited by  $\text{H}_2$  buildup in ADM1 (Batstone et al. 2002). However, this last strategy led to  $\text{H}_2$  accumulation in the gas phase (i.e. 2 - 5 %, data not shown), though no  $\text{H}_2$  was detected experimentally. Therefore, all the VFA-degrading populations might be affected in some degree by  $\text{NH}_3$  accumulation, as suggested by Poggi-Varaldo et al. (1997).

The model suggested a 5 - 15 % difference between the simulated and experimental TS and VS contents, despite the experimental trends were well approximated in both cases [Figure 4d]. Therefore, since the simulated  $M_{\text{Global}}$ ,  $\text{CH}_4$  yield and COD showed good simulations, an experimental bias was suspected in the experimental TS/VS measurement. Noteworthy, the recalculated TS and VS [Equations 19 to 21] improved considerably the matching of the TS and VS simulations with the values observed experimentally, though some differences were also observed from day 20 onwards. Meanwhile, the TS and VS recalculation is supported by the fact that some organic material (i.e. VFA), ammonia nitrogen (i.e.  $\text{NH}_3$ ) and/or inorganic carbon (i.e.  $\text{CO}_2$ ) might volatilize when drying the samples at 105 °C for prolonged periods of time (i.e. 24 h) (Angelidaki et al. 2009, EPA 2001). With all the above, the observed differences between the TS and VS recalculated and experimental values [Figure 4d] were likely related to the differences in the propionate and valerate simulations [Figure 4b] during the same period. Therefore, the model calibration might require further improvement as also discussed in next section.

500

### 501 3.2.2 Need for Further Calibration

502 The model calibration in this study was aimed to be minimal because of: 1) the  
503 complexity of HS-AD vs. the assumptions taken (i.e. homogenized reactor); 2) the little  
504 data available regarding solids mass dynamics (i.e. TS/VS); 3) the high number of  
505 biochemical parameters involved (i.e. > 10); and 4) the ‘strong’ interrelationship  
506 between parameters and the initial conditions in structured AD models (Batstone et al.  
507 2015, Donoso-Bravo et al. 2011, Flotats et al. 2010, Vanrolleghem et al. 1995). Thus,  
508 the calibration in this study was mainly addressed to the simultaneous fitting of the  
509 overall dynamics of TS/VS removal, reactor mass, biogas production, VFA and pH, in  
510 order to assess the potentiality of the proposed model to simulate a homogenized HS-  
511 AD matrix.

512 The parameter modification compared to ADM1 values [Table 4] was needed to obtain  
513 an adequate fitting of the overall set of experimental data for the sacrifice test in this  
514 study. Importantly, most of the biochemical parameters modified were within the  
515 recommended range suggested in ADM1, with the exception of the maximum  
516 propionate and valerate growth rates (i.e.  $k_{m,pro}$  and  $k_{m,va}$ ) that could be associated to  
517  $NH_3$  inhibition, as mentioned in section 3.2.1. For example, the lower and upper pH  
518 levels for acetate uptake ( $pH_{LL,ac}$  and  $pH_{UL,ac}$ , respectively) might vary around 30 %  
519 from the values proposed in ADM1 (i.e.  $pH_{LL,ac} = 6.0$  and  $pH_{UL,ac} = 7.0$ ) (Batstone et al.  
520 2002). However, it must be highlighted that the implementation of a single experimental  
521 dataset was not enough to calibrate a large number of parameters since, for example,  
522 different combinations of biochemical parameters and/or initial conditions (i.e.  
523 microorganisms) could yield practically the same agreement between experimental and  
524 simulated results (Girault et al. 2011, Jablonski and Lukaszewicz 2014, Vanrolleghem  
525 et al. 1995, Vavilin et al. 2008). Therefore, more experimental datasets (i.e. laboratory

526 and/or large scale applications) are needed to refine the calibration of the proposed  
527 parameters for HS-AD of OFMSW. Meanwhile, a sensitivity analysis and an adequate  
528 parameter optimization strategy might reveal important aspects about the main  
529 biochemical and physicochemical processes occurring in HS-AD of OFMSW.  
530 With all the above, the minimal model calibration showed the potentiality of using  
531 adequately the mass balances alongside the biochemical framework of ADM1 to  
532 simulate HS-AD of OFMSW. Thus, the HS-AD model simulates particularly well the  
533 TS, VS, and  $M_{\text{Global}}$  dynamics of HS-AD, provided the four preliminary hypotheses  
534 proposed are fulfilled. Meanwhile, further studies are needed in order to improve the  
535 biochemical calibration of the HS-AD model, with the aim to explore the different  
536 acidification/inhibitory mechanisms of HS-AD fed with OFMSW. Further calibration  
537 will be also helpful to double check the hypotheses used, assess the HS-AD model  
538 performance and/or highlight potential areas requiring further model development.  
539 Summarizing, the user could calibrate the model parameters and/or readapt the HS-AD  
540 model structure as required for any particular HS-AD application.

541

#### 542 **4 CONCLUSIONS**

543 In this study, a novel ADM1-based model was developed to simulate the solids and  
544 reactor mass/volume dynamics of homogenized HS-AD reactors. An adequate mass  
545 balance implementation condensed the effects of biogas production on HS-AD  
546 mass/volume, being critical to simulate relatively long operations. Apparent  
547 concentrations accounted for the TS concentration effect on soluble species. The model  
548 was verified for 'wet' AD and HS-AD, serving as a link between both operational  
549 regimes. The model simulated particularly well HS-AD of OFMSW in batch, including

550 the TS and reactor mass, while further model calibration might serve to assess

551 inhibitory mechanisms in HS-AD of OFMSW.

552

553 **Acknowledgements**

554 This project has received funding from the European Union's Horizon 2020 research

555 and innovation programme under the Marie Skłodowska-Curie grant agreement No.

556 643071. The authors thank Ulf Jeppsson for his inestimable comments when verifying

557 the ADM1 implementation.

558 **REFERENCES**

- 559
- 560 Abbassi-Guendouz, A., Brockmann, D., Trably, E., Dumas, C., Delgenes, J.P., Steyer,  
561 J.P. and Escudie, R. (2012) Total solids content drives high solid anaerobic  
562 digestion via mass transfer limitation. *Bioresour. Technol.* 111, 55-61.
- 563 Angelidaki, I. and Ahring, B.K. (1993) Thermophilic anaerobic digestion of livestock  
564 waste: the effect of ammonia. *Appl. Microbiol. Biotechnol.* 38(4), 560-564.
- 565 Angelidaki, I., Alves, M., Bolzonella, D., Borzacconi, L., Campos, J.L., Guwy, A.J.,  
566 Kalyuzhnyi, S., Jenicek, P. and van Lier, J.B. (2009) Defining the biomethane  
567 potential (BMP) of solid organic wastes and energy crops: a proposed protocol for  
568 batch assays. *Water Sci. Technol.* 59(5), 927-934.
- 569 ASTM (2002) D854-02: Standard test methods for specific gravity of soil solids by  
570 water pycnometer, ASTM International, American Society for Testing and  
571 Materials, United States.
- 572 Batstone, D.J. (2006) Mathematical modelling of anaerobic reactors treating domestic  
573 wastewater: rational criteria for model use. *Rev. Environ. Sci. Bio.* 5(1), 57-71.
- 574 Batstone, D.J., Keller, J., Angelidaki, I., Kalyuzhnyi, S.V., Pavlostathis, S.G., Rozzi, A.,  
575 Sanders, W.T., Siegrist, H. and Vavilin, V.A. (2002) The IWA Anaerobic  
576 Digestion Model No. 1 (ADM1). *Water Sci. Technol.* 45(10), 65-73.
- 577 Batstone, D.J., Puyol, D., Flores-Alsina, X. and Rodríguez, J. (2015) Mathematical  
578 modelling of anaerobic digestion processes: applications and future needs. *Rev.*  
579 *Environ. Sci. Bio.* 14(4), 595-613.
- 580 Benbelkacem, H., Bollon, J., Bayard, R., Escudié, R. and Buffière, P. (2015) Towards  
581 optimization of the total solid content in high-solid (dry) municipal solid waste  
582 digestion. *Chem. Eng. J.* 273, 261-267.
- 583 Benbelkacem, H., Garcia-Bernet, D., Bollon, J., Loisel, D., Bayard, R., Steyer, J.P.,  
584 Gourdon, R., Buffiere, P. and Escudie, R. (2013) Liquid mixing and solid  
585 segregation in high-solid anaerobic digesters. *Bioresour. Technol.* 147, 387-394.
- 586 Blumensaat, F. and Keller, J. (2005) Modelling of two-stage anaerobic digestion using  
587 the IWA Anaerobic Digestion Model No. 1 (ADM1). *Water Res.* 39(1), 171-183.
- 588 Bollon, J., Benbelkacem, H., Gourdon, R. and Buffière, P. (2013) Measurement of  
589 diffusion coefficients in dry anaerobic digestion media. *Chem. Eng. Sci.* 89, 115-  
590 119.
- 591 Cecchi, F., Pavan, P., Battistoni, P., Bolzonella, D. and Innocenti, L. (2002)  
592 Characteristics of the organic fraction of municipal solid wastes in Europe for  
593 different sorting strategies and related performances of the anaerobic digestion  
594 process, Mérida, Yucatán.
- 595 Chen, Y., Cheng, J.J. and Creamer, K.S. (2008) Inhibition of anaerobic digestion  
596 process: a review. *Bioresour. Technol.* 99(10), 4044-4064.
- 597 De Baere, L. (2000) Anaerobic digestion of solid waste: state-of-the-art. *Water Sci.*  
598 *Technol.* 41(3), 283-290.
- 599 De Baere, L. and Mattheeuws, B. (2013) *Waste Management: Recycling and Recovery.*  
600 Thomé-Kozmiensky Karl J., T.S. (ed), pp. 517-526.
- 601 De Gracia, M., Sancho, L., García-Heras, J.L., Vanrolleghem, P. and Ayesa, E. (2006)  
602 Mass and charge conservation check in dynamic models: application to the new  
603 ADM1 model. *Water Sci. Technol.* 53(1), 225-240.

- 604 Donoso-Bravo, A., Mailier, J., Martin, C., Rodriguez, J., Aceves-Lara, C.A. and Vande  
605 Wouwer, A. (2011) Model selection, identification and validation in anaerobic  
606 digestion: a review. *Water Res.* 45(17), 5347-5364.
- 607 EPA (2001) Method 1684. Total, fixed and volatile solids in water, solids, and  
608 biosolids., U.S. Environmental Protection Agency (EPA), Washington, DC.
- 609 Flotats, X., Palatsi, J., Fernandez, B., Colomer, M.A. and Illa, J. (2010) Identifying  
610 anaerobic digestion models using simultaneous batch experiments. *Environ.*  
611 *Engineer. Manag. J.* 9(3), 313-318.
- 612 Gallert, C. and Winter, J. (1997) Mesophilic and thermophilic anaerobic digestion of  
613 source-sorted organic wastes: effect of ammonia on glucose degradation and  
614 methane production. *Appl. Microbiol. Biotechnol.* 48, 405-410.
- 615 Girault, R., Rousseau, P., Steyer, J.P., Bernet, N. and Béline, F. (2011) Combination of  
616 batch experiments with continuous reactor data for ADM1 calibration: application  
617 to anaerobic digestion of pig slurry. *Water Sci. Technol.* 63(11), 2575.
- 618 Henze, M., Harremoës, P., Jansen, J.I.C. and Arvin, E. (1997) Wastewater treatment.  
619 Biological and chemical processes, Springer, Berlin.
- 620 Jablonski, S.J. and Lukaszewicz, M. (2014) Mathematical modelling of methanogenic  
621 reactor start-up: importance of volatile fatty acids degrading population.  
622 *Bioresour. Technol.* 174, 74-80.
- 623 Jokela, J.P. and Rintala, J. (2003) Anaerobic solubilisation of nitrogen from municipal  
624 solid waste (MSW). *Rev. Environ. Sci. Bio.* 2, 67-77.
- 625 Kayhanian, M. (1995) Biodegradability of the organic fraction of municipal solid waste  
626 in a high-solids anaerobic digester. *Waste Manage. Res.* 13, 123-136.
- 627 Kayhanian, M. (1999) Ammonia inhibition in high-solids biogasification: an overview  
628 and practical solutions. *Environ. Technol.* 20(4), 355-365.
- 629 Kayhanian, M. and Hardy, S. (1994) The impact of four design parameters on the  
630 performance of a high-solids anaerobic digestion of municipal solid waste for fuel  
631 gas production. *Environ. Technol.* 15(6), 557-567.
- 632 Kayhanian, M. and Tchobanoglous, G. (1996) Development of a mathematical model  
633 for the simulation of the biodegradation of organic substrates in a high-solids  
634 anaerobic digestion. *J. Chem. Tech. Biotechnol.* 66, 312-322.
- 635 Kell, G.S. (1975) Density, thermal expansivity, and compressibility of liquid water from  
636 0 to 150°C: Correlations and tables for atmospheric pressure and saturation  
637 reviewed and expressed on 1968 temperature scale. *J. Chem. Eng. Data* 20(1), 97-  
638 105.
- 639 Kleerebezem, R. and van Loosdrecht, M.C.M. (2006) Critical analysis of some concepts  
640 proposed in ADM1. *Water Sci. Technol.* 54(4), 51-57.
- 641 Lide, D.R. (2004) Handbook of chemistry and physics, CRC Press.
- 642 Mata-Alvarez, J. (2003) Biomethanization of the organic fraction of municipal solid  
643 wastes, IWA Publishing, London, UK.
- 644 Mata-Alvarez, J., Macé, S. and Llabrés, P. (2000) Anaerobic digestion of organic solid  
645 wastes. An overview of research achievements and perspectives. *Bioresour.*  
646 *Technol.* 74(1), 3-16.
- 647 Pavan, P., Battistoni, P., Mata-Alvarez, J. and Cecchi, F. (2000) Performance of  
648 thermophilic semi-dry anaerobic digestion process changing the feed  
649 biodegradability. *Water Sci. Technol.* 41(3), 75-81.

- 650 Poggi-Varaldo, H.M., Valdés, L., Esparza-García, F. and Fernández-Villagómez, G.  
 651 (1997) Solid substrate anaerobic co-digestion of paper mill sludge, biosolids, and  
 652 municipal solid waste. *Water Sci. Technol.* 35(2-3), 197-204.
- 653 Rajagopal, R., Masse, D.I. and Singh, G. (2013) A critical review on inhibition of  
 654 anaerobic digestion process by excess ammonia. *Bioresour. Technol.* 143, 632-  
 655 641.
- 656 Richards, B.K., Cummings, R.J., White, T.E. and Jewell, W.J. (1991) Methods for  
 657 kinetic analysis of methane fermentation in high solids biomass digesters.  
 658 *Biomass Bioenergy* 1(2), 65-73.
- 659 Rodríguez, J., Lema, J.M., van Loosdrecht, M.C.M. and Kleerebezem, R. (2006)  
 660 Variable stoichiometry with thermodynamic control in ADM1. *Water Sci.*  
 661 *Technol.* 54(4), 101-110.
- 662 Rosén, C. and Jeppsson, U. (2006) Aspects on ADM1 implementation within the BSM2  
 663 framework., Division of Industrial Electrical Engineering and Automation,  
 664 Faculty of Engineering, Lund University, Sweden.
- 665 van Veen, J.A. and Paul, E.A. (1979) Conversion of biovolume measurements of soil  
 666 organisms, grown under various moisture tensions, to biomass and nutrient  
 667 content. *Appl. Environ. Microbiol.* 37(4), 686-692.
- 668 Vanrolleghem, P., Van Daele, M. and Dochain, D. (1995) Practical identifiability of  
 669 biokinetic model of activated sludge respiration. *Water Res.* 29(11), 2561-2570.
- 670 Vavilin, V.A. and Angelidaki, I. (2005) Anaerobic degradation of solid material:  
 671 importance of initiation centers for methanogenesis, mixing intensity, and 2D  
 672 distributed model. *Biotechnol. Bioeng.* 89(1), 113-122.
- 673 Vavilin, V.A., Fernandez, B., Palatsi, J. and Flotats, X. (2008) Hydrolysis kinetics in  
 674 anaerobic degradation of particulate organic material: an overview. *Waste*  
 675 *Manage.* 28(6), 939-951.
- 676 Vavilin, V.A., Lokshina, L.Y., Jokela, J.P. and Rintala, J.A. (2004) Modeling solid  
 677 waste decomposition. *Bioresour. Technol.* 94(1), 69-81.
- 678 Vavilin, V.A., Rytov, S.V., Lokshina, L.Y., Pavlostathis, S.G. and Barlaz, M.A. (2003)  
 679 Distributed model of solid waste anaerobic digestion: effects of leachate  
 680 recirculation and pH adjustment. *Biotechnol. Bioeng.* 81(1), 66-73.
- 681 Xu, F., Li, Y. and Wang, Z.-W. (2015) Mathematical modeling of solid-state anaerobic  
 682 digestion. *Prog. Energy Combust. Sci.* 51, 49-66.

683  
 684  
 685 **Table 1:** Biochemical kinetics used for model implementation verification and  
 686 calibration.

687 **Table 2:** Influent and initial conditions used for model implementation verification and  
 688 model calibration.

689 **Table 3:** Summary of steady-state results for model implementation verification.

690 **Table 4:** Main parameters modified for model calibration.

691

692 **Figure 1:** High-solids vs. 'wet' anaerobic digestion.

693 **Figure 2:** Schematic representation of the high-solids anaerobic digestion model  
 694 implementation.

695 **Figure 3:** Hydraulic retention time and organic loading rate in model implementation  
 696 verification: a) 'wet' anaerobic digestion (simulations A and B); and b) high-solids  
 697 anaerobic digestion (simulations C and D).

698 **Figure 4:** Batch mono-digestion of OFMSW at 15 % total solids: a) accumulated  
699 methane production and reactor mass content; b) volatile fatty acids; c) total and free  
700 ammonia nitrogen; and d) total and volatile solids.  
701  
702

ACCEPTED MANUSCRIPT



1 **Table 1:** Biochemical kinetics used for model implementation verification and  
 2 calibration.  
 3

Process	Rate ( $\rho_j$ , kg COD $m^{-3} d^{-1}$ )	
	Model Verification	Model Calibration
Disintegration	$k_{dis} * X_c$	-
Hydrolysis of Carbohydrates	$k_{h,ch} * X_{ch}$	$k_{h,ch} * X_{ch}$
Hydrolysis of Proteins	$k_{h,pr} * X_{pr}$	$k_{h,pr} * X_{pr}$
Hydrolysis of Lipids	$k_{h,li} * X_{li}$	$k_{h,li} * X_{li}$
Sugars Uptake	$k_{m,su} * S_{su,App} / (K_{S,Xsu} + S_{su,App}) * X_{su} * I_{pH} * I_{in}$	$k_{m,su} * S_{su,App} / (K_{S,Xsu} + S_{su,App}) * X_{su} * I_{pH} * I_{in}$
Aminoacids Uptake	$k_{m,aa} * S_{aa,App} / (K_{S,Xaa} + S_{aa,App}) * X_{aa} * I_{pH} * I_{in}$	$k_{m,aa} * S_{aa,App} / (K_{S,Xaa} + S_{aa,App}) * X_{aa} * I_{pH} * I_{in}$
LCFA Uptake	$k_{m,fa} * S_{fa} / (K_{S,Xfa} + S_{fa}) * X_{fa} * I_{pH} * I_{in} * I_{h2}$	$k_{m,fa} * S_{fa} / (K_{S,Xfa} + S_{fa}) * X_{fa} * I_{pH} * I_{in} * I_{h2}$
Valerate Uptake	$k_{m,c4} * S_{va,App} / (K_{S,Xc4} + S_{va,App}) * X_{c4} * S_{va,App} / (1 + S_{bu,App} + 10^6 * I_{pH} * I_{in} * I_{h2})$	$k_{m,c5} * S_{va,App} / (K_{S,Xc5} + S_{va,App}) * X_{c5} * I_{pH} * I_{in} * I_{h2}$
Butyrate Uptake	$k_{m,c4} * S_{bu,App} / (K_{S,Xc4} + S_{bu,App}) * X_{c4} * S_{bu,App} / (1 + S_{bu,App} + 10^6 * I_{pH} * I_{in} * I_{h2})$	$k_{m,c4} * S_{bu,App} / (K_{S,Xc4} + S_{bu,App}) * X_{c4} * I_{pH} * I_{in} * I_{h2}$
Propionate Uptake	$k_{m,pro} * S_{pro,App} / (K_{S,Xpro} + S_{pro,App}) * X_{pro} * I_{pH} * I_{in} * I_{h2}$	$k_{m,pro} * S_{pro,App} / (K_{S,Xpro} + S_{pro,App}) * X_{pro} * I_{pH} * I_{in} * I_{h2}$
Acetate Uptake	$k_{m,ac} * S_{ac,App} / (K_{S,Xac} + S_{ac,App}) * X_{ac} * I_{pH} * I_{in} * I_{nh3}$	$k_{m,ac} * S_{ac,App} / (K_{S,Xac} + S_{ac,App}) * X_{ac} * I_{pH} * I_{in} * I_{nh3}$
Hydrogen Uptake	$k_{m,h2} * S_{h2,App} / (K_{S,Xh2} + S_{h2,App}) * X_{h2} * I_{pH} * I_{in}$	$k_{m,h2} * S_{h2,App} / (K_{S,Xh2} + S_{h2,App}) * X_{h2} * I_{pH} * I_{in}$
Sugar Degraders Decay	$k_d * X_{su}$	$k_d * X_{su}$
Aminoacids Degraders Decay	$k_d * X_{aa}$	$k_d * X_{aa}$
LCFA Degraders Decay	$k_d * X_{fa}$	$k_d * X_{fa}$
Valerate Degraders Decay	-	$k_d * X_{c5}$
Butyrate Degraders Decay	$k_d * X_{c4}$	$k_d * X_{c4}$
Propionate Degraders Decay	$k_d * X_{pro}$	$k_d * X_{pro}$
Acetate Degraders Decay	$k_d * X_{ac}$	$k_d * X_{ac}$
Hydrogen Degraders Decay	$k_d * X_{h2}$	$k_d * X_{h2}$

4 with

$$I_{in} = S_{in,App} / (K_{S,Sin} + S_{in,App})$$

$$I_{h2} = K_{i,S_{h2}} / (K_{i,S_{h2}} + S_{h2,App})$$

$$I_{pH} = K_{pH} * N_{pH} / (K_{pH} * N_{pH} + S_{h+} * N_{pH})$$

$$I_{nh3} = K_{i,S_{nh3}} / (K_{i,S_{nh3}} + S_{nh3,App})$$

5

1 **Table 2:** Influent and initial conditions used for model implementation verification and  
 2 model calibration.  
 3

Name	Model Verification			Model Calibration	Units
	Simulation A	Simulation B	Simulations C & D		
$S_{su}$	0.010	0.010	0.010	13.557	kg COD m <sup>-3</sup>
$S_{aa}$	0.001	0.001	0.001	2.207	kg COD m <sup>-3</sup>
$S_{fa}$	0.001	0.001	0.001	1.393	kg COD m <sup>-3</sup>
$S_{va}$	0.001	0.001	0.001	0.734	kg COD m <sup>-3</sup>
$S_{bu}$	0.001	0.001	0.001	0.500	kg COD m <sup>-3</sup>
$S_{pro}$	0.001	0.001	0.001	2.059	kg COD m <sup>-3</sup>
$S_{ac}$	0.001	0.001	0.001	0.103	kg COD m <sup>-3</sup>
$S_{h2}$	1.000E-08	1.000E-08	1.000E-08	1.000E-08	kg COD m <sup>-3</sup>
$S_{ch4}$	1.000E-08	1.000E-08	1.000E-08	1.000E-08	kg COD m <sup>-3</sup>
$S_{ic}$	0.040	0.040	0.040	0.029	kmol C m <sup>-3</sup>
$S_{in}$	0.010	0.010	0.010	0.186	kmol N m <sup>-3</sup>
$S_i$	0.020	0.020	0.020	0.000	kg COD m <sup>-3</sup>
$S_{i,subs}$	-	-	-	32.227	kgCOD m <sup>-3</sup>
$X_c$	2.000	2.000	2.000	-	kg COD m <sup>-3</sup>
$X_{ch}$	5.000	5.000	120.000	40.671	kg COD m <sup>-3</sup>
$X_{pr}$	20.000	20.000	20.000	30.902	kg COD m <sup>-3</sup>
$X_g$	5.000	5.000	5.000	12.534	kg COD m <sup>-3</sup>
$X_{su}$	0.010	0.010	0.010	0.050	kg COD m <sup>-3</sup>
$X_{aa}$	0.010	0.010	0.010	0.050	kg COD m <sup>-3</sup>
$X_{fa}$	0.010	0.010	0.010	0.001	kg COD m <sup>-3</sup>
$X_{c5}$	-	-	-	0.010	kgCOD m <sup>-3</sup>
$X_{c4}$	0.010	0.010	0.010	0.002	kg COD m <sup>-3</sup>
$X_{pro}$	0.010	0.010	0.010	0.005	kg COD m <sup>-3</sup>
$X_{ac}$	0.010	0.010	0.010	0.003	kg COD m <sup>-3</sup>
$X_{h2}$	0.010	0.010	0.010	0.070	kg COD m <sup>-3</sup>
$X_i$	25.000	25.000	250.000	0.000	kg COD m <sup>-3</sup>
$X_{i,subs}$	-	-	-	80.567	kgCOD m <sup>-3</sup>
$S_{cat}$	0.040	0.040	0.040	0.100	kmoleq m <sup>-3</sup>
$S_{an}$	0.020	0.020	0.020	0.051	kmoleq m <sup>-3</sup>
$\rho_{Global}$	-	1000.000	1100.000	1077.633	kg m <sup>-3</sup>
TS	-	4.500	25.000	15.502	%
VS	-	3.500	23.000	12.942	%

1 **Table 3:** Summary of steady-state results for model implementation verification.

Variable	ADM1 Implementation		HS-AD Model Implementation			Units
	Rosen & Jeppsson (2006)	'Wet' AD	'Wet' AD Const. Effluent**	HS-AD Const. Effluent**	HS-AD Variable Effluent	
$S_{su}$	0.01195	0.01195	0.01269	0.01692	0.01000	kg COD m <sup>-3</sup>
$S_{ac}$	0.19763	0.19721	0.27484	0.16339	0.05707	kg COD m <sup>-3</sup>
$S_{ic}$	0.15268	0.15270	0.15232	0.11377	0.11028	kmole C m <sup>-3</sup>
$S_{in}$	0.13023	0.13023	0.13129	0.08451	0.07803	kmole N m <sup>-3</sup>
$X_{ch}$	0.02795	0.02795	0.03183	60.73693	41.21685	kg COD m <sup>-3</sup>
$X_{su}$	0.42017	0.42017	0.43628	5.38786	6.15898	kg COD m <sup>-3</sup>
$X_{ac}$	0.76056	0.76058	0.78837	2.35994	2.52894	kg COD m <sup>-3</sup>
$Q_{Effluent}$	170	170	170	170	160	m <sup>3</sup> d <sup>-1</sup>
pH	7.47	7.46	7.48	7.20	7.16	m <sup>3</sup> d <sup>-1</sup>
$S_{co2}$	0.0099	0.0099	0.0096	0.0128	0.0134	kmol C m <sup>-3</sup>
$S_{nh3}$	0.0041	0.0041	0.0042	0.0015	0.0012	kmol N m <sup>-3</sup>
$P_T$	1.069	1.069	1.069	1.180	1.220	bar
$Q_g$	2956	2956	2939	9752	12472	Nm <sup>3</sup> d <sup>-1</sup>
%CH <sub>4</sub>	61*	60.9	60.8	50.6	49.9	%
%CO <sub>2</sub>	34*	33.9	34.0	44.7	45.5	%
$V_{Global}$	3400	3400	2967	1717	3400	m <sup>3</sup>
$\rho_{Global0}$	-	1000	1000	1100	1100	kg m <sup>-3</sup>
$\rho_{Global}$	-	1000	995	1082	1077	kg m <sup>-3</sup>
HRT	20*	20	20	20	20	d
HRT <sub>real</sub>	-	20	17	10	20	d
OLR	-	2.85	2.85	19.85	19.85	kg COD m <sup>-3</sup> d <sup>-1</sup>
OLR <sub>real</sub>	-	2.85	3.27	39.32	19.86	kg COD m <sup>-3</sup> d <sup>-1</sup>
TS <sub>0</sub>	4.5*	-	4.5	25.0	25.0	%
TS	-	-	2.9	20.4	19.0	%
TS <sub>Recalc</sub>	-	-	1.9	19.8	18.5	%
VS <sub>0</sub>	-	-	3.5	23.0	23.0	%
VS	-	-	1.8	18.2	16.9	%
VS <sub>Recalc</sub>	-	-	0.9	17.6	16.3	%

\*Mentioned Only; \*\*No Steady-State Reached.

2  
3  
4

1 **Table 4:** Main parameters modified for model calibration.

Parameter	ADM1	This Study	Units
$k_{h,ch}$	10	0.05	$d^{-1}$
$k_{h,pr}$	10	0.05	$d^{-1}$
$k_{h,li}$	10	0.07	$d^{-1}$
$k_{m,su}$	70	35	$d^{-1}$
$k_{m,fa}$	10	4	$d^{-1}$
$k_{m,c5}$	30	1	$d^{-1}$
$k_{m,c4}$	30	6	$d^{-1}$
$k_{m,pro}$	20	1	$d^{-1}$
$pH_{LL,ac}$	6	5.8	
$pH_{UL,ac}$	7	6.8	
$f_{bu,su}$	0.13	0.37	
$f_{pro,su}$	0.27	0.11	
$f_{ac,su}$	0.41	0.40	
$f_{h2,su}$	0.19	0.12	
$N_{i,subs}$	-	0.001	$kmol\ N\ m^{-3}$

2

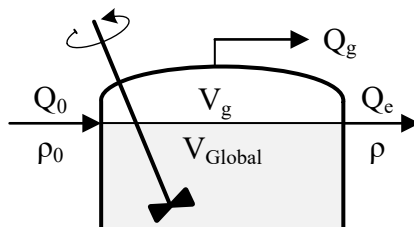
3

**‘Wet’ Anaerobic Digestion**

$$Q_0 = Q_e = Q$$

$$V_{\text{Global}} = \text{const.}$$

$$V_{\text{Global}} \frac{d\rho}{dt} = Q(\rho_0 - \rho) - \sum r_i$$

**High-Solids Anaerobic Digestion**

$$Q_0 \neq Q_e$$

$$V_{\text{Global}} \neq \text{const.}$$

$$\frac{d(\rho V_{\text{Global}})}{dt} = \rho_0 Q_0 - \rho Q_e - \sum r_i$$

**Figure 1:** High-solids vs. ‘wet’ anaerobic digestion.

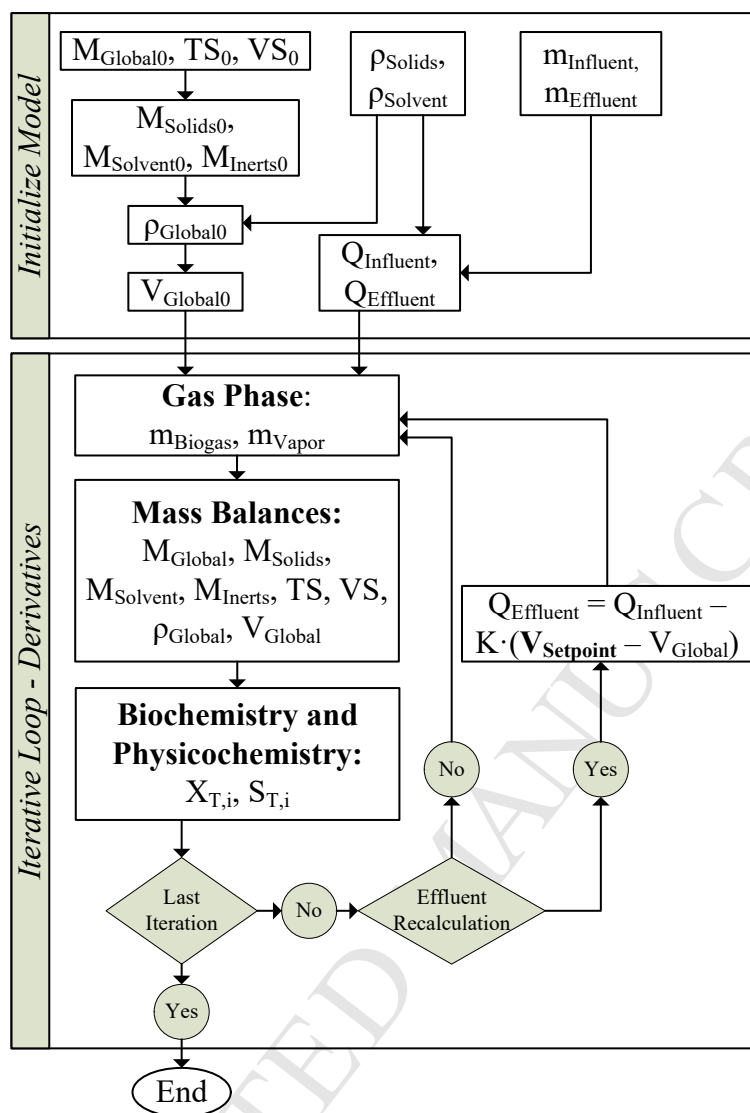


**Figure 2:** Schematic representation of the high-solids anaerobic digestion model implementation.

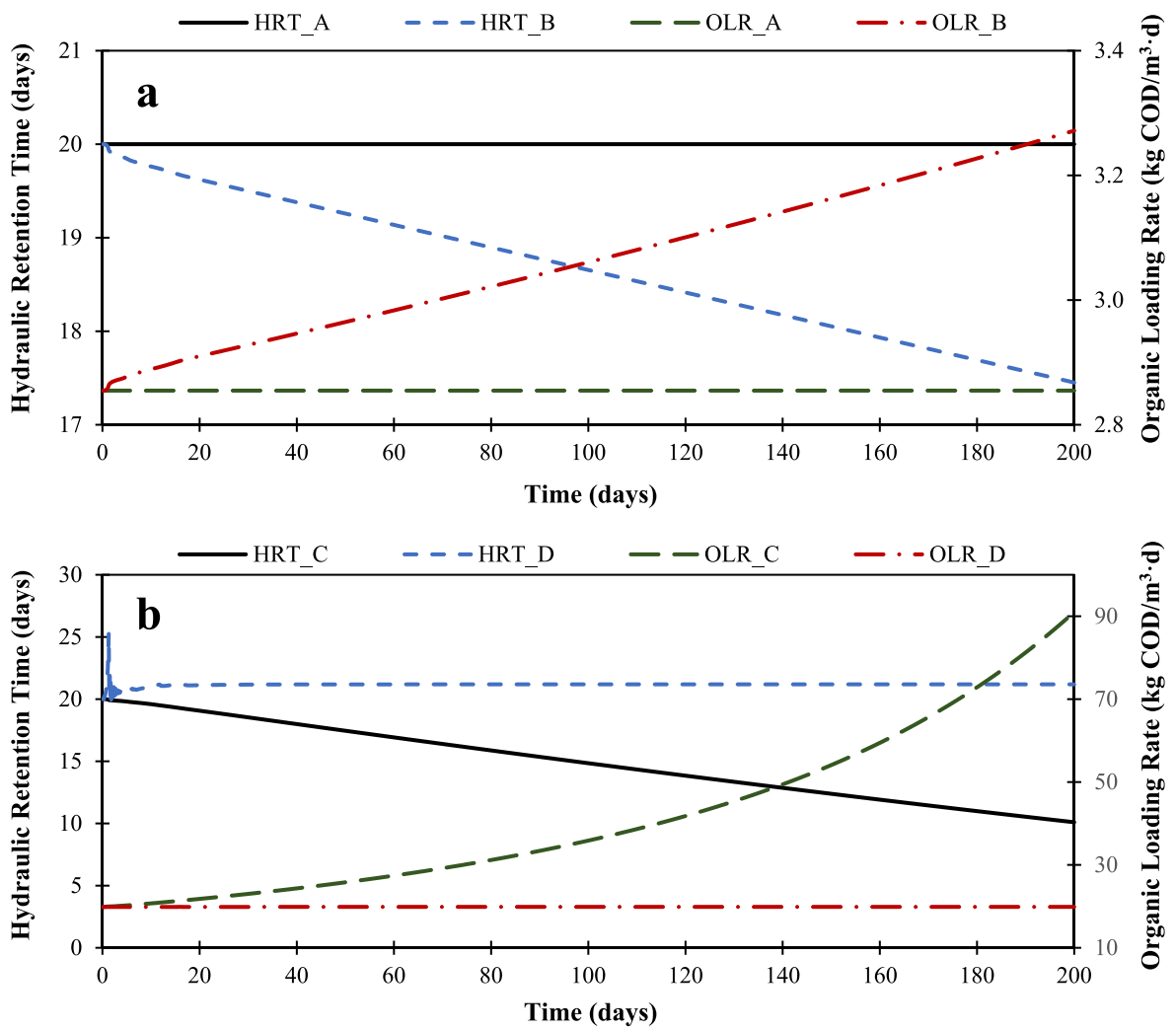


**Figure 3:** Hydraulic retention time and organic loading rate in model implementation verification: a) 'wet' anaerobic digestion (simulations A and B); and b) high-solids anaerobic digestion (simulations C and D).

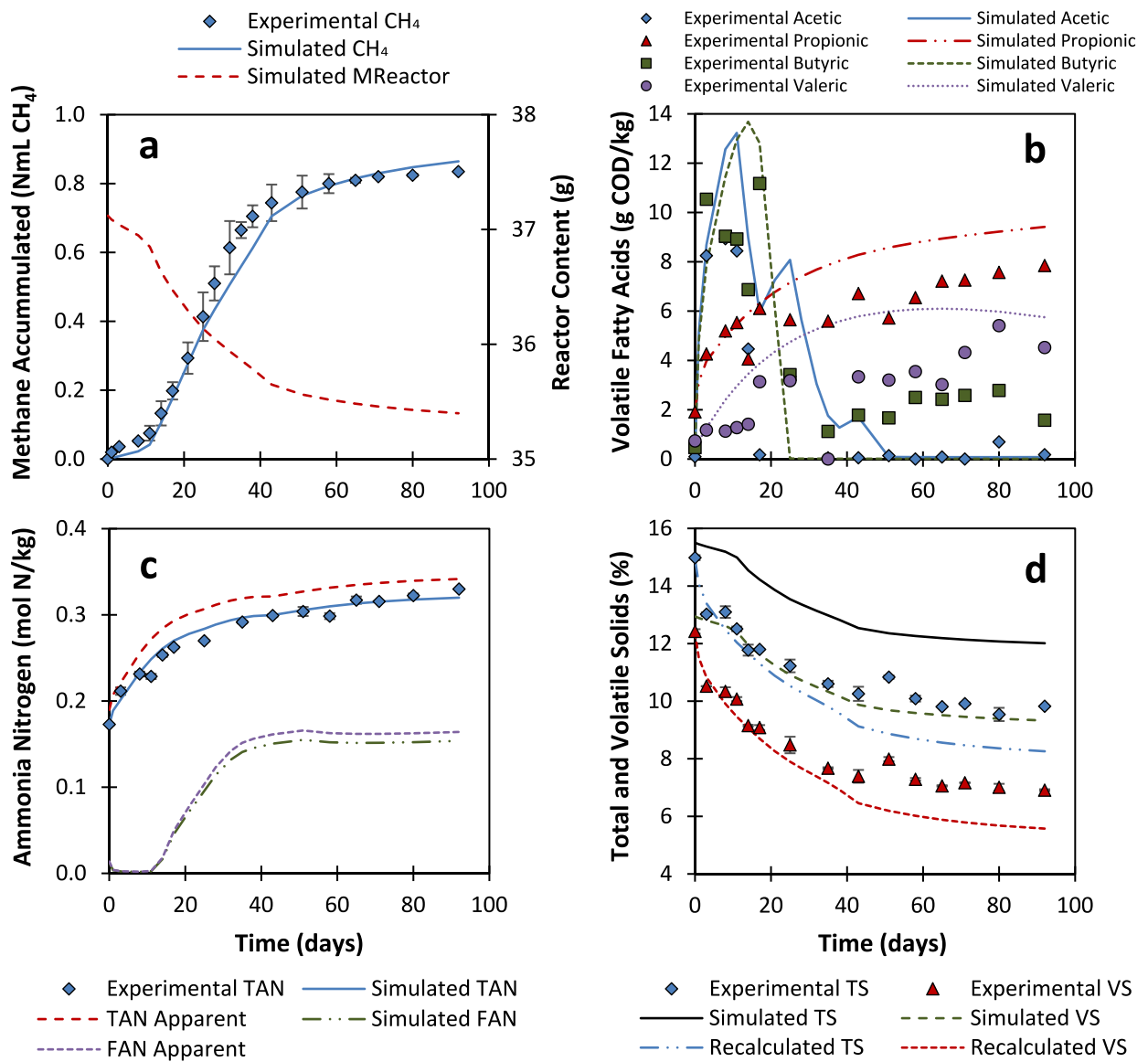


**Figure 4:** Batch mono-digestion of OFMSW at 15% total solids: a) accumulated methane production and reactor mass content; b) volatile fatty acids; c) total and free ammonia nitrogen; and d) total and volatile solids.



**Highlights**

- A novel HS-AD model based on ADM1 was developed for homogenized reactors.
- Reactor mass/volume and total solids dynamics in HS-AD were simulated.
- The model considers the TS concentration effect on soluble species in HS-AD.
- The model simulated adequately VFA and TAN of HS-AD using OFMSW as substrate.